Closed Loop Torque and Speed Control of Switched Reluctance Motor for Hybrid Electrical Vehicle Propulsion

Mohamed YAICH

Laboratory of Electronic Systems & Sustainable Energy (ESSE)
University of Sfax, National School of Engineers- B.P 1173, 3038 Sfax, Tunisia.

Yaich_fr2000@yahoo.fr

Mohamed Radhouan HACHICHA

Laboratory of Electronic Systems & Sustainable Energy (ESSE)
University of Sfax, National School of Electronics and Telecommunications.
B.P 1163, 3018 Sfax, Tunisia.

radhouan.mail@gmail.com

Moez GHARIANI

Laboratory of Electronic Systems & Sustainable Energy (ESSE)
University of Sfax, National School of Electronics and Telecommunications.
B.P 1163, 3018 Sfax, Tunisia.

moez.ghariani@gmail.com

Rafik Neji

Laboratory of Electronics and Information Technology (LETI)
Electric Vehicle and Power Electronics Group (VEEP)
University of Sfax, National School of Engineers- B.P 1173, 3038 Sfax, Tunisia.
Rafik.neji@gmail.com

***Abstract*-- Switched reluctance motors "SRMs" are gaining interest as a potential candidate for Hybrid Electric Vehicle "HEV" propulsion. SRM is a doubly-salient, singly excited machine and having very simple construction. It has a low inertia and allows an extremely high-speed operation. The control system of SRM is highly complex due to non linear nature; however these merits are overshadowed by its inherent high torque ripple, acoustic noise and difficulty to control. In this work, modeling, simulation and analysis of Switched Reluctance motor has been done. Various models of Switched reluctance Motor control strategies are simulated in MATLAB/SIMULINK. The control strategies used are PI Control, Hysteresis Control and voltage control. The result obtained from simulation has been presented. The control signal and circuit design for operation of a Switched Reluctance Motor (SRM) drive has been described.**

Index Terms--switched reluctance motor, PI Control, Hysteresis Control and voltage control, Hybrid Vehicle.

1. INTRODUCTION

The power electronic converters and electric propulsion motors are crucial components for modern hybrid electric vehicle (HEV). Accordingly, it is necessary that the associated traction motor and drive, operate at their optimal effectiveness throughout the test cycle. In typical HEV propulsion the electric motor is used over the entire operating range of torque / speed. SRMs are beginning to gain interest as a potential candidate for HEV propulsion due to their simple and rugged construction, fault tolerant operation, insensitivity to high temperatures, an extremely long constant-power range and high speed operation [1]-[2]. In this motor only the stator has got windings. The rotor contains no conductors or permanent magnets [3]. It consists simply of steel laminations stacked onto a shaft. It is because of this simple mechanical construction SRMs carry the promise of low cost, which in turn has motivated a large amount of research on SRMs in the last decade [4]. The motor speed-torque characteristics are also excellently matching with the road load characteristics [5]-[10], and the performance of SRM for HEVs applications has been found to be excellent. However, there are several barriers that need to be resolved before they can be applied in mass produced vehicles [11]-[14]. Since SRM involves successive excitation of poles to produce Continuous motoring or generating torque by aligning the rotor, the motor drive needs a position sensor for high-grade control. Torque ripple, vibration and associated acoustic noise are also the main concerns in SRM operation [15]-[17]. These issues are critical in vehicle application and research is targeted towards analysis, design improvement and development of excitation schemes and control strategies to reduce these effects. With the High concern over the energy resource crisis and global warming, Hybrid Electric Vehicle (HEVs) has become the most suitable candidate for the next generation vehicle due to their lower emission, high fuel efficiency. For the HEV, electric motor is one of the most important devices which should be reliable, robust, powerful, highly efficient and low cost. The electric drive-train comprises battery, motor, converter and control algorithm. Due to the variable DC bus voltage caused by the variation in the state of charge (SOC) of the battery and the nonlinearities found both in the motor and the switching converter, the torque control for switched reluctance motor while optimizing the motor efficiency for traction application becomes very complex. Extensive works have been done to optimize the efficiency of SRM at high speeds. The manufacturing cost of the SRM is relatively low and it can be operated at very high speed without mechanical problems.

2. SRM CHRACTERISTICS

The SRM has the simplest structure of any electric machine. It is a doubly-salient and singly-excited reluctance machine with independent phase windings on the stator, which is usually made of magnetic steel laminations. The rotor is a simple stack of laminations, without any windings or magnets. The basic 3-phase SRM structure has 6 stator and 4 rotor poles within the single stator geometry as shown in Figure 1. Each stator and rotor pole has pole arc of 30˚ mechanical. The stator windings on diametrically opposite poles are connected either in series or in parallel to form one phase of the motor. When a stator phase is energized, the most adjacent rotor pole-pair is attracted toward the energized stator to minimize the reluctance of the magnetic path. Therefore, by energizing consecutive phases in succession, the SRM develops reluctance torque in either direction of rotation. Fig.1 shows its linear inductance profile L(θ) with each phase inductance displaced by an angle θ_s given by inductance profile of each phase.

TABLE I

Specifications of SRM

S.NO	PARAMETER	VALUE
1	Stator Resistance	0.05 ohms
2	Inertia	0.05 Kg.m.m
3	Friction	0.02 N*m*s
4	Initial Speed and Position	[0,0](rad/s, theta)
5	Rotor Angle Vector	[0 10 20 30 40 45]
6	Stator Current Vector	0:25:450

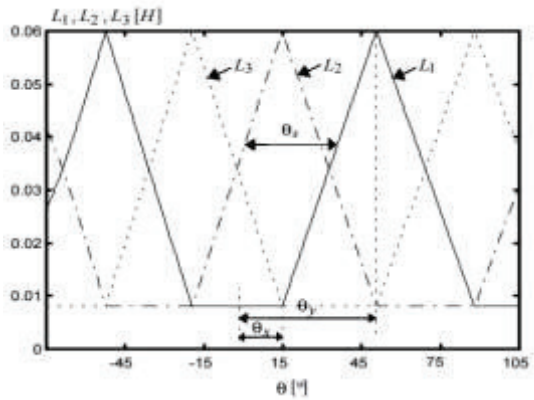

Fig. 1. SRM linear model. Inductance profile of each phase.

$$J\frac{\partial\omega}{\partial t}=\Gamma-\Gamma_l-f\omega \qquad (9)$$

Where Γ_l represents the torque load, and f the machine friction coefficient.

$$\theta_s=2\pi\left(\frac{1}{N_r}-\frac{1}{N_s}\right) \qquad (1)$$

Where N_r and N_s are the number of rotor and stator poles, respectively. When the motor has equal rotor and stator pole arcs, $\beta_r = \beta_s$, we get the following angle relations:

$$\theta_x=\left(\frac{\pi}{N_r}-\beta_r\right) \qquad (2)$$

$$\theta_y=\frac{\pi}{N_r} \qquad (3)$$

Fig. 2 shows the angle δ corresponding to the displacement of a phase in relation to another, which is given by

$$\delta=2\pi\left(\frac{1}{N_r}-\frac{1}{N_s}\right) \qquad (4)$$

The studied 6/4 SRM has the following parameters:
$L_{min} = 8$ mH, $L_{max} = 60$ mH , and $\beta_r = \beta_s = 30°$. Thus, from (2) and (3), we get $\theta_x = 15°$ and $\theta_y = 45°$.
The electric equation of each phase is given by:

$$\frac{\partial\psi_{i(\theta,I_i)}}{\partial t}+RI_i=V \qquad (5)$$

With $i = \{1, 2, 3\}$

While excluding saturation and mutual inductance effects, the flux in each phase is given by the following linear equation:

$$\psi_{i(\theta,I_i)}=L(\theta)I_i \qquad (6)$$

The total energy associated with the three phases (n = 3) is given by:

$$W_{total}=\frac{1}{2}\sum_{i=1}^{3}L\left(\theta+(n-i-1)\theta_s\right)I_i^2 \qquad (7)$$

and the motor total torque by:

$$\Gamma=\frac{1}{2}\sum_{i=1}^{3}\frac{\partial L\left(\theta+(n-i-1)\theta_s\right)}{\partial\theta}I_i^2 \qquad (8)$$

The mechanical equations are:
The angular velocity can be written as follows :

$$\frac{\partial\theta}{\partial t}=\omega \qquad (10)$$

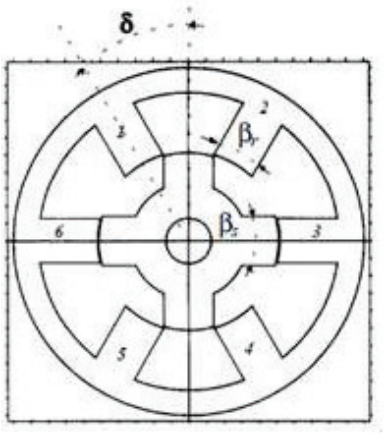

Fig. 2 . The angle δ corresponding to displacement of a phase in relation to another

We show in Fig. 3 the simulation diagram used for the SRM simulation using Simulink, which is the use of conventional blocks allowing understanding the programmed structure more easily.
Fig. 4 shows the content of the block phase 1. It contains four other blocks, each one associated with a specific Matlab function. The complete model can be used in application of Hybrid Electric Vehicle with proper turning on/off of the operating mode region of SRM/Gs

3. SRM ENERGIZING STRATEGIES

The torque developed in a SRM is independent of the direction of current flow. Thus unipolar converters are sufficient to serve as the power converter circuit for the SRM, unlike induction motors or synchronous motors that require bidirectional currents to flow through the power devices.

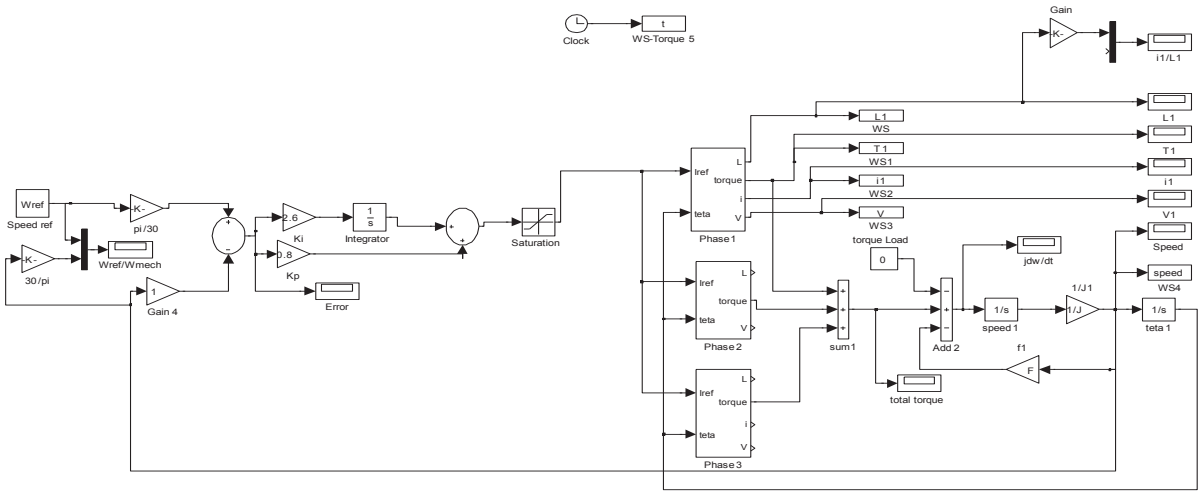

Fig. 3. Matlab/Simulink diagram of SRM linear model

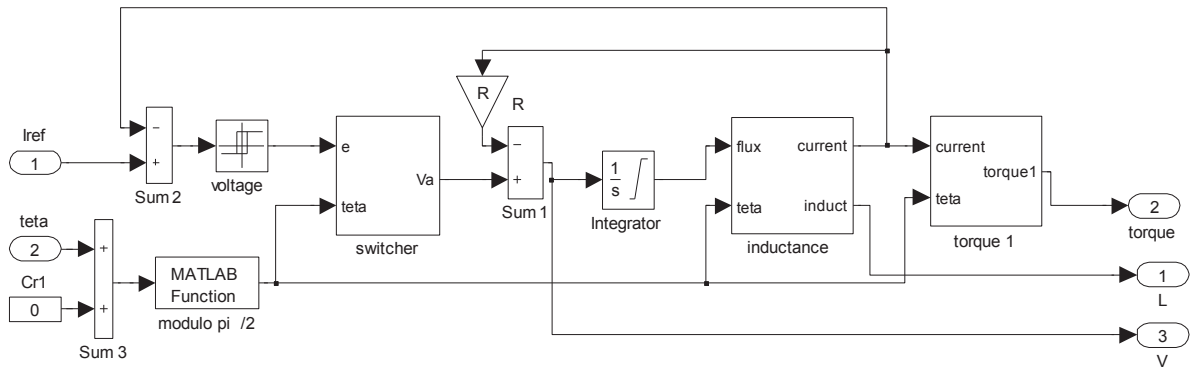

Fig.4.Block phase 1.

The fact that stator phases are electrically isolated has generated a wide variety of converter configurations [18]. The type of the converter required for a particular SRM drive application is intimately related to motor construction and the number of phases.

The SRM has the added advantage of reduced hysteresis losses due to the unidirectional current flow. The converter circuit supplies the required pulsed waveforms from a DC source for the operation of the SRM. The most flexible and versatile four-quadrant SRM is the classic bridge converter topology, which has two transistors and two freewheeling diodes per phase as shown in Figure 5 [19]. The transistor switches are turned ON and OFF in each phase depending on controller outputs for torque and speed control of the SRM.

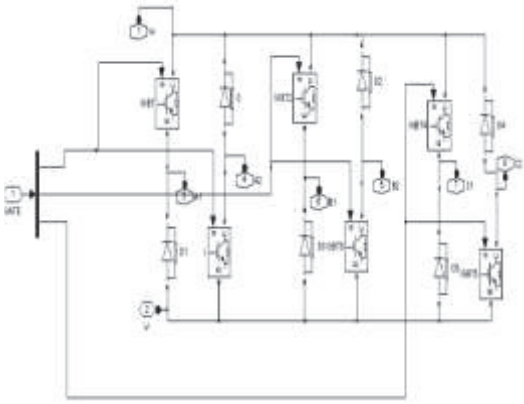

Fig. 5. H-bridge asymmetric converter

Assuming linearity, the flux relation is given by:

$$\psi = L(\theta) I \tag{11}$$

The co-energy is given by:

$$W = L(\theta) I^2 \tag{12}$$

Resulting in a torque given by:

$$\Gamma = \frac{1}{2} \frac{\partial L}{\partial \theta} I^2 \tag{13}$$

Expression (13) shows that this converter is unidirectional in current because torque production does not depend on the current sign but only on $\frac{\partial L}{\partial \theta}$ sign.

4. SRM CONTROLLEUR STRATEGIES

The effective performance characteristics from a SRM drive system can be obtained by proper positioning of the phase excitation pulses relative to the rotor position. The commutation angles (turn-on angle θ_{on}, turn-off angle θ_{off}), total conduction period and the magnitude of the phase current (I_{ref}) determine the average torque, torque ripple and other performance parameters. The difficulty to find the control parameters depends on the chosen control method for a particular application. At low speeds, the current rises almost instantaneously after turn-on because of the negligible back-emf and the current must be limited by either controlling the average voltage or by regulating the current level. As the speed increases, the back-emf increases and opposes the applied bus voltage. Phase advancing is necessary to establish the phase current at the onset of rotor and stator pole overlap region. Voltage PWM or chopping control is used to force maximum current into the motor to maintain the desired torque level. The torque command is executed by regulating the current in the inner loop as shown in the closed-loop block diagram in Figure 6. The desired current "I_{ref}", is dependent upon the load characteristics, speed and control strategy. The simpler control strategy is to generate one current command to be used by all the phases in succession. The electronic switch selects the appropriate phase for current regulation based on θon, θoff and the instantaneous rotor position. The current controller generates the gating signal for the power devices based on the information coming from the electronic switch. With both the switches turned ON, the energizing current in the phase winding increases with positive DC-link voltage. For current control, the switches are operated to freewheel, magnetize and demagnetize depending on the rotor position and direction. The current in the switched phase is quickly brought to zero applying "-Vdc", while the incoming phase ensures the torque production depending on the used current. The torque ripple tends to increase since the torque production is not smooth during phase transition in these drives. Usually, three kinds of current controllers are used for the SRM, namely: PI controller, hysteresis controller and hybrid structure which is a combination of the first two.

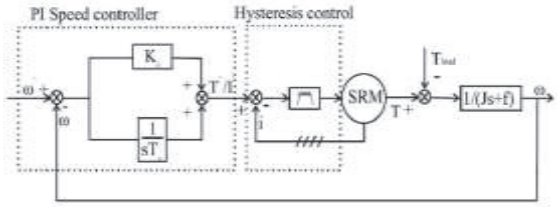

Fig.6. Closed-loop speed and current control block diagram of a SRM.

In this project, the hysteresis current controller is used for its simplicity [20]. There are many choices for the outer speed controller, such as PID controller, two degree of freedom controller, fuzzy controller, adaptive controller, and artificial neural

network controller. The PI controller is used in this research for simplicity.

A.Closed loop current controller design

Current feedback is essential for this proposed control strategy. Here each of the phase-currents are sensed and fed back to controller. A hysteresis controller is used to control the phase current according to reference current generated by the speed controller. The only control parameter is the hysteresis band Δi. In the case of an analog implementation, this parameter ensures that the instantaneous current is bounded between i∗ ±Δi/2, where i∗ is the desired current. In this case, the current ripple is equal to Δi and the current controller output takes only two distinct values ± Vdc. Its generates switching pulses by comparing reference current and sensed current as mentioned below:
If, Iact < I_{Lw} , switch is turned on.
and Iact > I_{Up}, switch is turned off.

B. Speed control loop

The PI controlleur parameters calculated according a small signal model of the SRM drive sustem, to satisfy the control specification. Transfer function of the PI controller is

$$G_{PI} = K_I \frac{\left(\frac{K_P}{K_I} + 1\right)}{S} \quad (14)$$

5. SIMULATIONS RESULTS

A PI controller is used for speed control of the SRM in simulation because of its simplicity. The advantage of the controller is that the speed of the machine can be controlled with fast transient without overshoots, and good steady state response as shown in Figure 3. The PI speed control loop is in the outer loop generating the desired phase current command based on the speed as shown in closed-loop block diagram of Figure 6. Here, the desired current "I_{ref}" is not fixed, but changes based on the error between the desired speed W_{ref} and actual machine speed W_m. The PI controller parameter values tuned in the simulation are: The proportional constant "$K_p = 0.8$" and the integral constant "$K_i = 0.03$".
With the motor functioning without load, waveforms can be obtained by integrating all the functional blocks in the motoring simulation figure 3 such as position wrapping, active phase determination, phase commutation and current regulation. Figure 7 shows inductance variation in SRM, which is considered as control reference for the phase commutation. The speed characteristic is shown in Figure 8. Figure 9 shows the total torque variation in time of all the three phases, the total electromagnetic torque is about 4 Nm. Torque ripple presents high magnitude for the used values of Turn-on (θon) and Turn-off (θoff) angles, having as consequence to originate important speed oscillations shown in figure 8. To decrease the speed oscillations it is necessary to produce more torque. Adjustment of the Turn-off angle value allowed fewer oscillations. However, ripple reduction is not an easy task because other parameters, such as the speed and load values, influence the torque ripple magnitude. Figure 10 gives the flux-linkage and gate signal of the converter phase PWM switching voltages for regulating the current in time. Here, the ripples are due to the current chopping control. The phase current is given in figure 11. It can be seen that the current flows only in the inductance rising slope as it is in motoring mode, also the phase current regulation between the turn-on and turn-off positions for motoring operation.

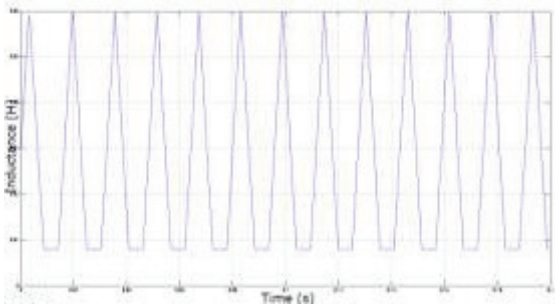

Fig. 7. Inductance profile

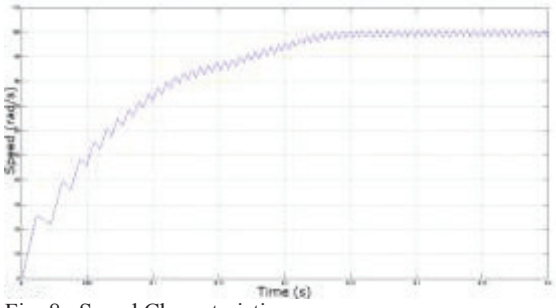

Fig. 8. Speed Characteristics

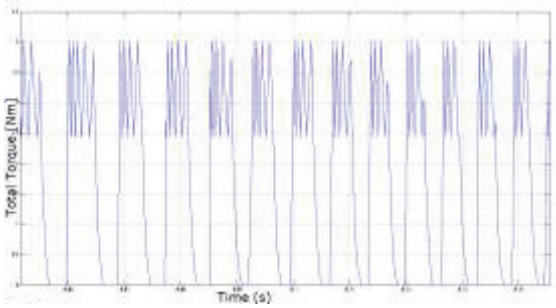

Fig.9. Total torque

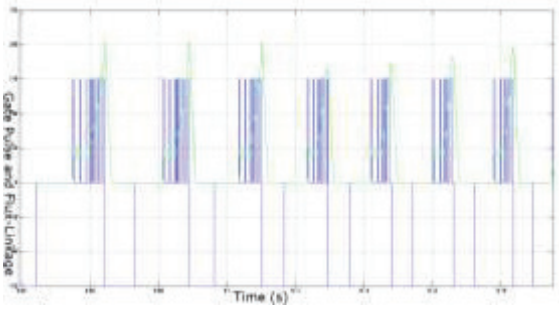

Fig.10. Gate Pulse and Flux-Linkage

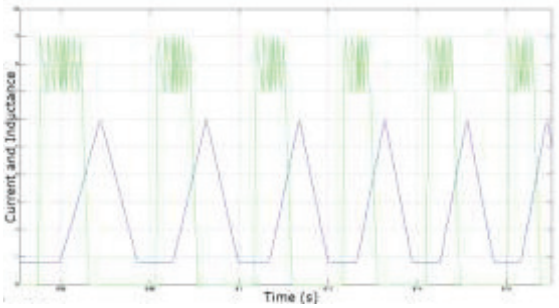

Fig. 11. Current and Inductance

6. CONCLUSION

Motivated by a desire to find an alternative vehicle which is independent on the petroleum, environment friendly and affordable, HEVs have been successfully launched commercially by major Car manufacturers. The performance of HEVs heavily relies on the development of drive-train, specifically, the traction motor. Hence, this research is focused on the torque control of SRM, which is one of the suitable traction motors for HEV application; we sought to reduce the torque ripple at low speeds and improve the power efficiency at high speeds. In this paper, mathematical modeling of SRM and advanced PI, as well as hysteresis controllers for SRM position control have been presented. The parameters of the speed PI controller are adjusted according to the load torque and rotor speed. The control scheme is based on the various converter topologies and it is capable for maintaining the torque ripple at an acceptable level over a wide speed range. It provides quick response and high-precision position control of the SRM. The proposed control scheme has been applied on a three-phase 6/4 SRM, with asymmetric converter topologies.

REFERENCES

[1] M. Krishnamurthy, C. S. Edrington, A. Emadi, P. Asadi, M. Ehsani, and B.Fahimi, "Making the case for applications of switched reluctance motor technology in automotive products," IEEE Trans. on Power Electronics, vol.21, pp. 659-675, May 2006.

[2] S. Wang, Q. Zhan, Z. Ma, and L. Zhou, "Implementation of a 50-kW four-phase switched reluctance motor drive system for hybrid electric vehicle," IEEE Trans. on Magnetics, vol. 41, part 2, pp. 501-504, Jan. 2005.

[3] Adrian David Cheok et al, (2002), "A New Torque and Flux Control Method for Switched Reluctance Motor Drives", IEEE Transaction on Power Electronics. Vol.17, No.4, pp. 543-557.

[4] T. J. E. Miller, "Switched Reluctance Motors and Their Control" Magna Physics Publishing and Clarendon Press, Oxford, 1993.

[5] Husain, Electric and Hybrid Vehicles – Design Fundamentals, Boca Raton: CRC Press, 2003

[6] K. M. Rahman, B. Fahimi, G. Suresh, A. V. Rajarathnam, and M. Ehsani,"Advantages of switched reluctance motor applications to EV and HEV: Design and control issues," IEEE Trans. on Industry Applications, vol. 36, pp. 111-121,Jan. -Feb. 2000

[7] D. -H. Lee, Z. -G. Lee, J. Liang, and J. -W. Ahn, "Single-phase SRM drive with torque ripple reduction and power factor correction," IEEE Trans. on Industry Applications, vol. 43, pp. 1578-1587, Nov. -Dec. 2007.

[8] H. Zhang, W. Xu, S. Wang, Y. Huangfu, G. Wang, and J. Zhu, "Optimum design of rotor for high-speed switched reluctance motor using level set method," IEEE Trans. Magn., vol. 50, no. 2, Feb. 2014.

[9] M. D. Hennen, R. W. D. Doncker, N. HFuengwarodsakul, and J. O. Fiedler, "Single-phase switched reluctance drive with saturation-based starting method," IEEETrans. Power Electron., vol. 26, no. 5, pp. 1337-1343, May 2011.

[10] K. Lu, U. Jakobsen, and P. O. Rasmussen, "Single-phase hybrid switched reluctance motor for low-power low-cost applications," IEEE Trans. Magn., vol. 47, no. 10, pp. 3288-3291, Oct. 2011.

[11] B. Bilgin, A. Emadi, and M, Krishnamurthy, "Design considerations for switched reluctance machines with a higher number of rotor poles," IEEE Trans. Ind. Electron., vol. 59, no. 10, pp. 3745-3756, Oct 2012.

[12] J. D. Widmer, and B. C. Mecrow, "Optimized segmental rotor switched reluctance machines with a greater number of rotor segments than stator slots," IEEE Trans. Ind. Appl., vol. 49, no. 4, pp. 1491-1498, Jul.-Aug. 2013.

[13] H. Eskandari, and M. Mirsalim, "An improved 9/12 two phase e-core switched reluctance machine," IEEE Trans. Energy Convers., vol. 28, no. 4, pp. 951-958, Dec. 2013.

[14] X. Liang, G. Li, J. Ojeda, M. Gabsi, and Z. Ren, "Comparative study of classical and mutually coupled switched reluctance motors using multiphysics finite-element modeling," IEEE Trans. Ind. Electron., vol. 61, no. 9, pp. 5066-5074, Sep. 2014.

[15] P. Andrada, B. Blanqué, E. Martínez, and M. Torrent, "A novel type of hybrid reluctance motor drive," IEEE Trans. Ind. Electron., vol. 61, no. 8, pp. 4337-4345, Aug. 2014.

[16] L. Shen, J. Wu, S. Yang, and X. Huang, "Fast flux linkage measurement for switched reluctance motors excluding rotor clamping devices and position sensors," IEEE Trans. Instrum. Meas., vol. 62, no. 1, pp. 185-191, Jan. 2013.

[17] H. Toda, K. Senda, S. Morimoto, and T. Hiratani, "Influence of various non-oriented electrical steels on motor efficiency and iron loss in switched reluctance motor," IEEE Trans. Magn., vol. 49, no. 7, pp. 3850-3853, Jul. 2013.

[18] Y. T. Chang, and K. W. E. Cheng, "Sensorless position estimation of switched reluctance motor at startup using quadratic polynomial regression," IET Electr. Power Appl., vol. 7, iss. 7, pp. 618-626, 2013.

[19] Y. Z. Xu, R. Zhong, L. Chen, and S. L. Lu, "Analytical method to optimise turn-on angle and turn-off angle for switched reluctance motor drives," IET Electr. Power Appl., vol. 6, iss. 9, pp.593-603, 2012.

[20] T. Ishikawa, Y. Hashimoto, and N. Kurita, "Optimum design of a switched reluctance motor fed by asymmetric bridge converter using experimental design method," IEEE Trans. Magn., vol. 50, no. 2, Feb. 2014.